

Exploiting null space potentials to control arm robots compliantly performing nonlinear tactile tasks

International Journal of Advanced
Robotic Systems
November-October 2019: 1–11
© The Author(s) 2019
DOI: 10.1177/1729881419885473
journals.sagepub.com/home/arx



Nikolas Wilhelm^{1,2} , Rainer Burgkart¹, Jan Lang^{1,2},
Carina Micheler^{1,2} and Constantin von Deimling^{1,2} 

Abstract

In this article, two new compliant control architectures are introduced that utilize null space solutions to decouple force and position control. They are capable to interact with uncertain surfaces and environments with varying materials and require fewer parameters to be tuned than the common architectures – hybrid or impedance control. The general concept behind these approaches allows to consider manipulators with six degrees of freedom as redundant by creating a virtual redundancy with a reduced work space. It will be demonstrated that the introduced approaches are superior regarding orthogonal separation of the Cartesian degrees of freedom and avoid inner singularities. To demonstrate their performance, the controllers are tested on a standard industrial robot (Stäubli, RX90B, six degrees of freedom) that actuates two different biomechanically inspired models of the human knee joint.

Keywords

Manipulator, interaction, haptic, contact tasks, constrained tasks, compliant control, force control, unknown or uncertain environments.

Date received: 2 August 2018; accepted: 20 September 2019

Topic Area: Robot Manipulation and Control

Topic Editor: Andrey V Savkin

Associate Editor: Jawhar Ghommam

Introduction

Due to the industrial need of robots performing tactile tasks, extensive research has been conducted on robot–object interaction in the past decades.¹ Although the key control strategies were established in the 1980s, the improvement of their accuracy, stability and robustness still challenges the robotic community today. In terms of haptic interactions, this is mainly caused by the task’s complexity itself: A non-linear robot is used to palpate surfaces or uncertain environments and is thereby non-linearly coupled to a partially unknown system.

Two broad categories of compliant or tactile control strategies deal with this task: hybrid position and force control methods. They divide the Cartesian task in force-regulated and position-controlled degrees of

freedom (DOFs)² and impedance control methods. The latter relate loads and displacements by a diagonal mass matrix combined with a regular damping and a stiffness matrix.³

¹Orthopaedic Research, Clinic for Orthopaedics and Sport Orthopaedics, Klinikum rechts der Isar, Technical University of Munich, Munich, Germany

²Department of Mechanical Engineering, Technical University of Munich, Munich, Germany

Corresponding author:

Constantin von Deimling, Orthopaedic Research, Clinic for Orthopaedics and Sport Orthopaedics, Klinikum rechts der Isar, Technical University of Munich, Ismaninger Str. 21 81675 München, Germany.

Email: constantin.deimling@tum.de



The drawback of impedance control methods is that neither position accuracy nor force precision are deterministic and that its stability is limited by the achievable impedances (z -width).^{4,5} Furthermore, they require parametrization of the unknown stiffness and damping matrix ($\in \mathbb{R}^{6 \times 6}$) which depend on the non-linear coupling between robot and environment. Newer implementations suggest the usage of observers like the extended Kalman filter to adapt the unknown and varying mechanical parameters.⁶ As a non-linear coupling between environment and robot remains and many parameters have to be estimated, hybrid methods tend to offer a decoupled solution with fewer parameters. However, they achieve decoupling in Cartesian space only. Their projection in joint space remains coupled. Moreover, the original hybrid approach is working with the Jacobian inverse making it vulnerable to inner singularities and therefore potentially unstable.⁷

To address these shortcomings, Khatib⁸ and Fisher and Mujtaba⁹ presented a different approach to dissection: Instead of dividing in Cartesian space and applying the original hybrid method, their method splits position and force-controlled DOFs into task and null space. Several authors following this idea of null space dissection presented various methods for kinematic^{10–14} and dynamic^{11,15–20} control summarized by Dietrich et al.²¹ However, while these approaches solve the coupling of the robot tasks, they still rely on the impedance approach with the discussed drawbacks. The framework of Schuetz et al.²² offers a new perspective as it combines tactile motion control with the decoupling solution of Fisher and Mujtaba.⁹ This allows to require few parameters only and to design the dynamics of the system. However, their method is only used to avoid obstacles and is insufficient for persistent contact. The specific usage of designing an explicit force controller based on this architecture has not been regarded yet offers a big potential for control approaches.

The two control methods presented in this article aim to address this gap by reformulating the framework of Schuetz et al.²² for explicit force control. They consist of a controller for single force or contact control, and one for multiple force control of partially or fully coupled nonlinear systems. As the inherited architecture is based on a null space separation,²² the control problem can be split according to the task priority. This prioritization increases the performance of the primary task as shown by Sandoval et al.²³ and therefore offers a greater flexibility.

The article is organized as follows. The fundamental framework is explained in the second section. The two new control methods are derived in the third section followed by a stability analysis and a proof, that the provided separation achieves complete decoupling in Cartesian and joint space. Further the prioritization technique is presented. A detailed presentation of our quantitative experiments is presented in the fourth section followed by the conclusion in the fifth section.

Related work

Within this section several related approaches to decoupled position and force control are presented and put in the context of our contribution.

Hybrid position/force control

One of the first compliant control architectures was the hybrid position/force control by Raibert and Craig.² The original idea behind this approach is to divide the Cartesian task into purely position- and force-regulated DOFs via the selector matrices \mathbf{S}_x and \mathbf{S}_f .² Both sets of position- $\delta\mathbf{x}$ and force- $\delta\mathbf{f}$ errors are controlled in parallel loops that project separately into joint space. These control loops are summed up as joint torques to receive the control torque τ_c .²

$$\tau_c = \mathbf{g}_x(\mathbf{S}_x\mathbf{J})^{-1}\delta\mathbf{x} + \mathbf{g}_f(\mathbf{S}_f\mathbf{J})^T\delta\mathbf{f} \quad (1)$$

with the Jacobian \mathbf{J} and the linear control functions \mathbf{g}_x and \mathbf{g}_f for the force- and position-control loop. The projections $(\mathbf{S}_x\mathbf{J})^{-1}$ and $(\mathbf{S}_f\mathbf{J})^T$ hereby map the position and torque error in joint space. Several authors showed that this kind of control scheme does lead to unstable robot behaviour outside the inner singularities.^{24,25} Fisher and Mujtaba⁹ demonstrated that a part of the stability issues are caused by the non-ideal separation of force and position DOFs. Although only certain degrees should be controlled by the position or force loop, the usage of the full rank Jacobian does lead to cross coupling. Therefore, Fisher and Mujtaba⁹ proposed projections by the reduced Jacobian. The Cartesian position error is projected by the identity-weighted pseudo-inverse⁸ of the position-selected Jacobian

$$(\mathbf{S}_x\mathbf{J})^\# = (\mathbf{S}_x\mathbf{J})^T(\mathbf{S}_x\mathbf{J}\mathbf{J}^T\mathbf{S}_x^T)^{-1} \quad (2)$$

while the force error is mapped by the transposed force selected Jacobian⁹

$$\tau_c = \mathbf{g}_x(\mathbf{S}_x\mathbf{J})^\#\delta\mathbf{x} + \mathbf{g}_f\left((\mathbf{S}_f\mathbf{J})^T\delta\mathbf{f}\right) \quad (3)$$

Although cross couplings are reduced by Fisher and Mujtaba's approach, it can be shown that force differences still lead to Cartesian velocities interfering with the position controlled DOFs. To minimize these effects, the null space offers meaningful solutions.

Null space solutions

In parallel to the historic development of hybrid position/force control, kinematic solutions for redundant robots emerged, whose number of joints n is larger than the number of DOFs m needed for the task ($n > m$). Besides the higher robustness of the inverse kinematic solution, they offer the possibility to perform additional tasks in null space. Therefore, the null space matrix \mathbf{N} is utilized. It is calculated by subtracting the product of the identity-

weighted pseudo-inverse⁸ $\mathbf{J}^\# \in \mathbb{R}^{n \times m}$ and the actual Jacobian $\mathbf{J} \in \mathbb{R}^{m \times n}$ from the unity matrix $\mathbf{I} \in \mathbb{R}^{n \times n}$. It represents the orthogonal projection of the Jacobian²⁶

$$\mathbf{N} = \mathbf{I} - \mathbf{J}^\# \mathbf{J} \quad (4)$$

Building on this projection any cost function $H(q)$ can be minimized in null space, using its gradient $\frac{\partial H(q)}{\partial q}$. According to Liégeois, the joint velocity is augmented by a gradient descent step with the stepsize α . The gradient is received by deriving the cost function with respect to the joints and projecting it into null space resulting in the null space control scheme²⁶

$$\dot{\mathbf{q}}_c = \mathbf{J}^\# \dot{\mathbf{x}}_t - \alpha \mathbf{N} \left(\frac{\partial H}{\partial \mathbf{q}} \right)^T \quad (5)$$

with the control joint velocity $\dot{\mathbf{q}}_c \in \mathbb{R}^n$ and the task space velocity $\dot{\mathbf{x}}_t \in \mathbb{R}^m$. Based on this framework, several control architectures were developed. They actually reduce impact forces or adjust a force step. Most of them are based on impedance control by Hogan³ and are implemented on acceleration level. Nemeč and Zlajpah introduced a hybrid impedance control for a 4-DOF arm robot. It utilizes the null space to react on impacts applied to the arm while maintaining the position and force at the tip in work space.²⁷ A similar approach is presented by Sadeghian et al. working with null space impedance and an observer to compensate impacts on a lightweight arm robot without force feedback.²⁸ Park and Khatib suggested a scheme which is capable to adjust two contact forces measured at the end-effector and a third applied to one of its links during velocity-commanded motions.²⁹ Platt et al. presented multi-priority impedance control, which fuses a Cartesian and a joint impedance via the null space to adjust a force step in one direction of the end-effector.³⁰ A recent approach by Sandoval et al. presents²³ a method for surgical application using the null space to apply constraints in favour of the patient's safety. Until now, no approach is known that separates force and position targets at the end-effector via the null space on velocity level and actually modulates forces while following position targets. To implement such a control architecture, tactile motion control by Schuetz et al. is adapted.²²

Tactile motion control

Influenced mainly by the works of Walker, Gertz et al. and Chung et al., Schuetz et al. extended (5) by three additional velocity inputs. These result from control in task, joint and null space ($\dot{\mathbf{u}}_t \in \mathbb{R}^m$, $\dot{\mathbf{u}}_j \in \mathbb{R}^n$ and $\dot{\mathbf{u}}_n \in \mathbb{R}^n$).^{7,22,31,32} They provide the opportunity to pursue additional tasks in work, joint and null space on velocity level

$$\begin{aligned} \dot{\mathbf{q}}_c &= \mathbf{J}^\# (\dot{\mathbf{x}}_t - \dot{\mathbf{u}}_t) - \dot{\mathbf{u}}_j \\ &\quad - \mathbf{N} \left(\dot{\mathbf{u}}_n + \alpha \left(\frac{\partial H}{\partial \mathbf{q}} \right)^T \right) \end{aligned} \quad (6)$$

Since the goal of this article is the separation of the task via the null space, it will recap the null space velocity extension $\dot{\mathbf{u}}_n$ only and physically interpret the approach. For simplicity, the cost function gradient as well as the additional joint- and task-space velocity are set to zero.²²

$$\dot{\mathbf{q}}_c = \mathbf{J}^\# \dot{\mathbf{x}}_t - \mathbf{N} \dot{\mathbf{u}}_n. \quad (7)$$

Like Walker, Schuetz et al. reduced the translatory three-dimensional contact phenomena to a one-dimensional equation.^{7,22} Consequently, the Jacobian $\mathbf{J} \in \mathbb{R}^{3 \times n}$ describes the translatory part of the general Jacobian at the tool centre point. Introducing the translatory Jacobian at the impact point $\mathbf{J}_p \in \mathbb{R}^{3 \times n}$ and the normalized force vector $\mathbf{n}_f \in \mathbb{R}^{3 \times 1}$, the direct kinematic relation³³ is used to transform (7) into contact space. Thereby, the one-dimensional contact space velocity \dot{x}_p is obtained

$$\begin{aligned} \dot{x}_p &= \mathbf{n}_f^T \mathbf{J}_p \dot{\mathbf{q}}_c \\ &= \mathbf{n}_f^T \mathbf{J}_p \mathbf{J}^\# \dot{\mathbf{x}}_t - \mathbf{n}_f^T \mathbf{J}_p \mathbf{N} \dot{\mathbf{u}}_n \end{aligned} \quad (8)$$

Schuetz et al. used the transposed Jacobian at the impact point \mathbf{J}_p^T and the normalized force vector. The velocity $\dot{\mathbf{u}}_n$ was projected to the force-driven velocity at the point of contact \dot{x}_f .

$$\dot{\mathbf{u}}_n = \mathbf{J}_p^T \mathbf{n}_f \dot{x}_f \quad (9)$$

Combining (8) and (9), the one-dimensional contact relation in Cartesian space at the contact point is obtained.²² To simplify this equation, the scalar velocity \dot{x}_{pt} and the kinematic variable k_n are introduced. \dot{x}_{pt} equals the main task velocity projected to contact space. k_n is a variable that describes the kinematic flexibility between null space and contact space

$$\dot{x}_p = \underbrace{\mathbf{n}_f^T \mathbf{J}_p \mathbf{J}^\# \dot{\mathbf{x}}_t}_{\dot{x}_{pt}} - \underbrace{\mathbf{n}_f^T \mathbf{J}_p \mathbf{N} \mathbf{J}_p^T \mathbf{n}_f}_{k_n} \dot{x}_f \quad (10)$$

By applying a linear elastic material law $\delta f_p = -c \delta x_p$ with a constant spring-coefficient c , the velocity at the contact point \dot{x}_p is related to the rate of the contact force vectorial norm \dot{f}_p .²²

$$\dot{f}_p = -c \dot{x}_{pt} + c k_n \dot{x}_f \quad (11)$$

Solving (11) for the force-driven velocity at the impact point and combining it with the projection from (9), the null space controller is received

$$\dot{\mathbf{u}}_n = \mathbf{J}_p^T \mathbf{n}_f \frac{1}{k_n} \underbrace{\left(\dot{x}_{pt} + \frac{\dot{f}_p}{c} \right)}_{\dot{x}_f} \quad (12)$$

Schuetz et al. suggest a linear second order dynamic with the dimensionless damping d and the time constant T to compute the force rate²²

$$\dot{f}_p = -\frac{2d}{T} f_p - \frac{1}{T^2} \int f_p t \quad (13)$$

Applying the dynamics of (13) to (12) gives the final control law for the null space force controller

$$\dot{\mathbf{u}}_n = \frac{\mathbf{J}_p^T \mathbf{n}_f}{ck_n} \left(c\dot{x}_{pt} - \frac{2d}{T} f_p - \frac{1}{T^2} \int f_p t \right) \quad (14)$$

In practice, a 9-DOF manipulator is enabled to reduce forces caused by the collision with its tactile hull.^{22,34} However, while this approach is sufficient for handling collision avoidance, it is not designed for persistent contact control or applying forces along multiple directions independently.

Null space divided compliant control

The contribution of this article is to combine the ideas of hybrid motion and tactile motion control. Firstly, the control law of Schuetz et al. is extended to palpate an undefined surface, while modulating forces normal to the plane. The control architecture is then extended to handle force control along multiple directions independently. We propose an additional null space exploitation by switching between position and force prioritization.

Contact control on an undefined surface

To achieve a sustained contact control with the desired dynamics, δf is defined as the scalar force error between the desired force f_d and the actual force at the tool centre point f_a

$$\delta f = f_d - f_a \quad (15)$$

Applying the second order dynamics to this force difference and solving for the actual force rate, equation (13) is extended for persisting contact

$$\dot{f}_a = \dot{f}_d + \frac{2d}{T} \delta f + \frac{1}{T^2} \int \delta f t \quad (16)$$

The scalar force rate at the contact point \dot{f}_p equals the actual force rate \dot{f}_a since the contact and the tool centre point coincide. Further, the Jacobian at the contact point \mathbf{J}_p does not differ any more from the one at tool centre point \mathbf{J} .

The motion around the surface is realized by the position loop in the main task. Therefore, the position-selected Jacobian \mathbf{J}_x is built

$$\mathbf{J}_x = \mathbf{S}_x \mathbf{J} \quad (17)$$

Recalculating the null space matrix of this reduced Jacobian N_x with (4) and inserting it in (12), the joint velocity is received with the modified projections

$$\dot{\mathbf{q}}_c = \mathbf{J}_x^\# \dot{\mathbf{x}}_t - N_x \dot{\mathbf{u}}_n \quad (18)$$

The main difference in the control setup occurs to the null space velocity input $\dot{\mathbf{u}}_n$ as it is extended according to the changed dynamics from (16):

$$\dot{\mathbf{u}}_n = \frac{\mathbf{J}_p^T \mathbf{n}_f}{ck_n} \left(c\dot{x}_{pt} + \dot{f}_d + \frac{2d}{T} \delta f + \frac{1}{T^2} \int \delta f t \right) \quad (19)$$

The result can be used as input for any joint control, which shows stable behaviour under the expected loading and velocities. It is only depending on three scalar parameters – time constant T , dimensionless damping d and stiffness c . The algorithm is suitable to palpate and load unknown surfaces or perform processing tasks, which need a modulated contact normal force to the surface. One possible application is painting a planarly defined logo on a curved surface.

Controlling multiple force directions

So far, the introduced framework concentrates on translatory motions on unknown surfaces. Consequently, the force is modulated in the direction of the reference force only. The framework is extended into Cartesian space to regulate forces in all directions. The idea behind this extension is to build a separated set of orthogonal contact control loops by projecting them along their corresponding axis. Therefore, we divide the normal force into a linear combination of its elements n_{f_x} , n_{f_y} , and n_{f_z}

$$\begin{aligned} \mathbf{n}_f &= \begin{pmatrix} n_{f_x} \\ 0 \\ 0 \end{pmatrix} + \begin{pmatrix} 0 \\ n_{f_y} \\ 0 \end{pmatrix} + \begin{pmatrix} 0 \\ 0 \\ n_{f_z} \end{pmatrix} \\ &= \mathbf{n}_{f_x} + \mathbf{n}_{f_y} + \mathbf{n}_{f_z} \end{aligned} \quad (20)$$

Null space velocity (9) changes to the following formulation and is now related to three direction-dependent and force-driven velocity inputs in Cartesian space \dot{x}_f , \dot{y}_f and \dot{z}_f

$$\dot{\mathbf{u}}_n = \mathbf{J}_p^T \left(\mathbf{n}_{f_x} \dot{x}_f + \mathbf{n}_{f_y} \dot{y}_f + \mathbf{n}_{f_z} \dot{z}_f \right) \quad (21)$$

Each of this velocities has its own kinematic variable that analogously calculates equation (10), exemplary shown for k_{n_y}

$$k_{n_y} = \mathbf{n}_{f_y}^T \mathbf{J}_p N_x \mathbf{J}_p^T \mathbf{n}_{f_y} \quad (22)$$

Applying the projection (10) equivalently and inserting the force component in normal direction, the scalar velocities at the tool centre point are resolved with the dynamics from (16)

$$\dot{y}_f = \frac{1}{ck_{n_y}} \left(c\dot{x}_{p_{ty}} + \dot{f}_{d_y} + \frac{2d}{T} \delta f_y + \frac{1}{T^2} \int \delta f_y t \right) \quad (23)$$

To analyse the kinematic relation between the joint velocities and the force component, the attained information from (23) and (22) is inserted into (21) exemplary for the y -related values

$$\begin{aligned} \dot{\mathbf{u}}_n &\propto \mathbf{J}_p^T \mathbf{n}_{f_y} \frac{1}{k_{n_y}} \dot{f}_{a_y} \\ &\propto \mathbf{J}_p^T \mathbf{n}_{f_y} \frac{1}{\mathbf{n}_{f_y}^T \mathbf{J}_p \mathbf{N}_x \mathbf{J}_p^T \mathbf{n}_{f_y}} \dot{f}_{a_y} \\ &\propto \frac{1}{n_{f_y}} \dot{f}_{a_y} \end{aligned} \quad (24)$$

Hence, it generates higher Cartesian velocities along the axes where the external force component is lower. This is especially useful if contact or resistance forces in the investigated direction exist. Otherwise, it leads to infinite velocities and thus has to be deactivated below a certain threshold

$$\lim_{n_y \rightarrow 0} \left(\frac{1}{n_{f_y}} \dot{f}_{a_y} \right) = \infty \quad (25)$$

The force-driven joint velocity in null space $\dot{\mathbf{q}}_n$ has to be low-pass filtered to produce smooth transitions. The proposed null space force control can be combined with any attitude control. Hybrid separation is solely implemented via null-space that is calculated over the selected Jacobian matrix \mathbf{J}_x . It filters any velocity component of the force loop, which interferes with the position control loop.

Stability

Based on the proof of stability by Sygulla et al. for tactile motion control, the two presented controllers are analysed.³⁴ Therefore, the dynamics from (16) are modified for contact (19) and multi-force (21) control, differentiated and solved for the corresponding control variable

$$\delta \ddot{f} = -\frac{2d}{T} \delta \dot{f} - \frac{1}{T^2} \delta f, \quad \text{if } A \quad (26)$$

$$\delta \ddot{f}_{\{x,y,z\}} = -\frac{2d}{T} \delta \dot{f}_{\{x,y,z\}} - \frac{1}{T^2} \delta f_{\{x,y,z\}}, \quad \text{if } B \quad (27)$$

with the boolean expressions

$$A := \{\text{Contact Control}\} \quad (28)$$

$$B := \{\text{Multi Force Control}\} \quad (29)$$

Both controllers meet the requirements of their designed target dynamics and are stable outside the Jacobian singularities.

Investigation of the decoupling

The proposed framework enables hybrid control on any joint-controlled robot which possesses a sufficient number of joints. This means that the number of joints does at least have to be as large as the dimension of the task space to be able to perform the task. With increasing number of joints, the null space is extended and the performance increases for the task applied to null space. The aim is to achieve a complete decoupling between position and force control in Cartesian space. Hybrid control as introduced by Raibert and Craig appears to offer a decoupled solution at first sight.² Yet, by applying the selector matrices \mathbf{S}_x and \mathbf{S}_f on the desired tasks in Cartesian space, the controllers are actually not really decoupled.⁹ They remain active along the non-selected DOFs and try to achieve zero velocity or zero loading, respectively, along those DOFs. The actual output of both control loops is concurrent and leads to decreasing performance. Therefore, a different approach to dissection has been taken by Fisher and Mujtaba,⁹ which is described in (3). Regarding joint velocity and introducing the position- and force-driven Cartesian velocities $\dot{\mathbf{x}}_x$ and $\dot{\mathbf{x}}_f$, it can be reformulated

$$\begin{aligned} \dot{\mathbf{q}}_c &= (\mathbf{S}_x \mathbf{J})^\# \dot{\mathbf{x}}_x + (\mathbf{S}_f \mathbf{J})^T \dot{\mathbf{x}}_f \\ &= \dot{\mathbf{q}}_x + \dot{\mathbf{q}}_f \end{aligned} \quad (30)$$

This equation consists of the position-driven and force joint velocity ($\dot{\mathbf{q}}_x$ and $\dot{\mathbf{q}}_f$). Transferring the joint velocities back to Cartesian space by the multiplication with the full Jacobian and looking only at the position-selected velocities. It can be recognized that force-driven velocities interact with position-selected ones

$$\begin{aligned} \mathbf{S}_x \mathbf{J} \dot{\mathbf{q}}_c &= \mathbf{S}_x \mathbf{J} (\mathbf{S}_x \mathbf{J})^\# \dot{\mathbf{x}}_x \\ &\quad + \mathbf{S}_x \mathbf{J} (\mathbf{S}_f \mathbf{J})^T \dot{\mathbf{x}}_f \end{aligned} \quad (31)$$

This can be proven by the dot product between the two addends which is in general not equal to zero. Therefore, the separation of Fisher and Mujtaba does not lead to orthogonal decoupled velocity components. Both control loops interact with each other within Cartesian space

$$(\mathbf{S}_x \mathbf{J} (\mathbf{S}_x \mathbf{J})^\# \dot{\mathbf{x}}_x) \cdot (\mathbf{S}_x \mathbf{J} (\mathbf{S}_f \mathbf{J})^T \dot{\mathbf{x}}_f) \neq 0 \quad (32)$$

In contrast to that, null space division implements an orthogonal split. Considering the syntax of the force- and position-driven Cartesian velocities, (18) is rewritten to a more general form

$$\dot{\mathbf{q}}_c = (\mathbf{S}_x \mathbf{J})^\# \dot{\mathbf{x}}_x + \mathbf{N}_x \mathbf{J}^T \dot{\mathbf{x}}_f \quad (33)$$

Repeating the projection of the position-selected Cartesian velocity and building the dot product, it can be seen that the velocities are split orthogonally. The dot product between the addends is equal to zero due to the definition of the null space matrix, which is the orthogonal projection of the position-selected Jacobian²⁶

$$\left(\mathbf{S}_x \mathbf{J} (\mathbf{S}_x \mathbf{J})^\# \dot{\mathbf{x}}_x \right) \cdot \left(\mathbf{S}_x \mathbf{J} \mathbf{N}_x \mathbf{J}^T \dot{\mathbf{x}}_f \right) = 0 \quad (34)$$

The orthogonality is also achieved in joint space.³⁵ Therefore, the dot product of the joint velocities is also equal to zero

$$\left((\mathbf{S}_x \mathbf{J})^\# \dot{\mathbf{x}}_x \right) \cdot \left(\mathbf{N}_x \mathbf{J}^T \dot{\mathbf{x}}_f \right) = 0 \quad (35)$$

Force prioritization

The usage of the null space matrix clearly improves the decoupling between the force and the position loop, but it also filters the magnitude of the signal multiplied with it. Consequently, the control's main task is prioritized higher than the secondary task.²¹ To investigate this effect, a corresponding force-prioritized control architecture is designed. It uses the null space matrix \mathbf{N}_f to filter out the position-controlled joint velocities not being orthogonal to the force-regulated ones

$$\dot{\mathbf{q}}_c = \mathbf{N}_f (\mathbf{S}_x \mathbf{J})^\# \dot{\mathbf{x}}_x + (\mathbf{S}_f \mathbf{J})^T \dot{\mathbf{x}}_f \quad (36)$$

The null-space matrix changes according to the force selection of the Jacobian

$$\mathbf{N}_f = \mathbf{I} - (\mathbf{S}_f \mathbf{J})^\# (\mathbf{S}_f \mathbf{J}) \quad (37)$$

Here, the force-controlled DOFs are operating in work space. While they have full access over the complete joint space, the position-controlled movements are filtered by \mathbf{N}_f . Neither the joint nor the Cartesian velocities are coupled. Their dot product is equal to zero.

$$\left(\mathbf{N}_f (\mathbf{S}_f \mathbf{J})^\# \dot{\mathbf{x}}_x \right) \cdot \left((\mathbf{S}_f \mathbf{J})^T \dot{\mathbf{x}}_f \right) = 0 \quad (38)$$

Experiments

Different experiments were conducted to gather information about the performance of the introduced control architectures. Their design concentrates on the two following aims:

- Determination of the contact and multi-force control's performance handling nonlinear compliant control tasks, and
- Analysis of the prioritization effects.

The performance is investigated by two different experiments or tasks that both are inspired by the biomechanical behaviour of the human knee joint. While the first experiment is designed to investigate the position-prioritized contact control, the second one is concentrated on the evaluation of the multi-force control and its force/position prioritization.



Figure 1. Experimental setup to evaluate the contact control. An additive manufactured femur replica is moved along a rigid oversized tibia plateau, which is cornered by rising edges.

Evaluation of the contact control

The contact control architecture is analysed during the palpation of an unknown surface. The tested unknown surface is an upscaled 3D-printed tibia (upper surface of the main lower leg bone) which can be assumed as a rigid body and is cornered by rising walls. Instead of a tool, the robot is attached to a femur model (upper leg bone). The setup is shown in Figure 1.

The evaluation task is to move along the shape of a logo on the surface of the upscaled tibia plateau while the compression force normal to the plateau is modulated along the edges. Regarding Cartesian space, this motion is defined by two translatory position-controlled DOFs and by the corresponding null space regulation of the compression force (see Figure 2). The force magnitude is defined to apply continuously varying compression forces in the range from 10 to 50 N in order to maintain contact. The force signal is low pass (PT1) filtered before processing with a time constant of the Cartesian position is changed via pentic splines, pausing at the logo's corners, with a referenced velocity maximum of 20 mm/s. The task's execution is visualized in the supplementary video. Although the velocity of the referenced trajectory is relatively high for a contact scenario, the contact control shows accurate position tracking. The maximal Euclidean norm of the position deviation $\delta x_{x,\max}$ is below 1.47 millimetres (mm). Its mean is 0.35 mm. The task's position trajectory is illustrated in Figure 3. In addition, the contact control shows precise

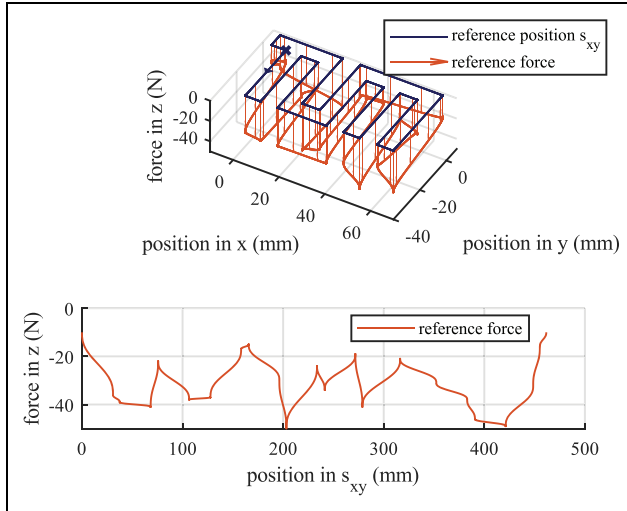


Figure 2. The contact control's evaluation task is to move along the surface of a logo, while modulating the perpendicular force along the edges.

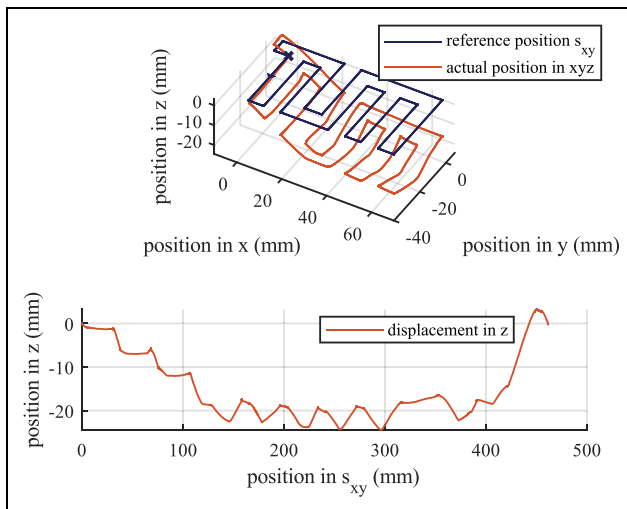


Figure 3. Displacement along the z-axis during the task movement. Visualized is the task trajectory s_{xy} and the actual trajectory in the first plot, as well as the vertical displacement along the task trajectory below.

force-tracking regarding the velocity as can be seen in Figure 4. The mean force error is 2.62 N. The maximum force error is 10.79 N. Since the higher force deviations occur when the contact point switches due to the shape of the femur condyles, lower reference velocities result in improved force tracking. Performing the same motion with half of the maximum velocity (10 mm/s), the mean force error can be reduced to 0.91 N. The maximum force error decreases to 6.89 N. The performance of the contact control is depending on a few already mentioned parameters. The control parameters were determined by performing a preliminary study in simulation containing 30 trials for each

Table I. Control parameters and quality measures of the contact control task.

Parameter	Value	Unit
Control frequency	4000	Hz
PT1-Force filter constant	0.04	s
Max. referenced velocity	20	mm s ⁻¹
PT2-Stiffness c	10.0	kN m ⁻¹
PT2-Damping d	1.2	s
PT2-Time constant T	0.16	s
Quality measure	Value	Unit
Position accuracy	<0.1	mm
Force accuracy	<0.1	N
Maximum Euclidean position error $\ \delta x\ _{\max}^2$	1.47	mm
Mean Euclidean position error $\ \delta x\ _{\text{mean}}^2$	0.35	mm
Maximum force deviation $ \delta f _{\max}$	12.35	N
Mean force deviation $ \delta f _{\text{mean}}$	2.53	N

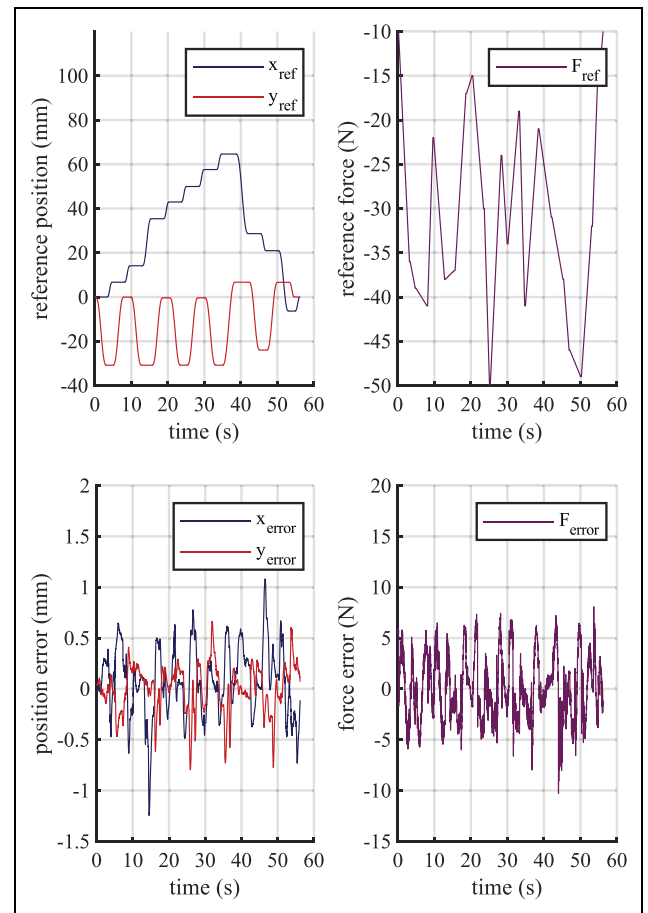


Figure 4. Path-following of the contact control.

experiment. These control parameters including the quality measures are summarized in Table 1.

Multi-force control with position prioritization

The multi-force control is investigated on the basis of a more comprehensive task. The robot actuates a



Figure 5. Test setup for the multi-force control. The robot is attached to an additive manufactured replica of the human knee joint.

biomechanical additive manufactured model of the human knee joint. The femur component is rigidly connected to the robot's tip. The tibia is fixed with the environment. In contrast to the model before, the tibia is original size and non-linearly coupled to the femur via ropes that mimic the collateral and cruciate ligaments (see Figure 5).

It is necessary to actuate the robot in different Cartesian degrees of freedom in order to identify the biomechanical characteristics of human joint specimens (e. g. range of motion). Loads orthogonal to the actively actuated DOFs have to be minimized. The task is to adjust the flexion angle actively while the force components' magnitudes are modulated in a range from 10 to 30 N. The position task is a one-dimensional rotation along the knee's flexion-axis from 0° to 11.5° . The remaining DOFs are used to modify the three-dimensional Cartesian forces in null space. The maximum angular velocity during the applied flexion is 2.75 deg s^{-1} .

The multi-force control is able to handle the described tasks, showing precise tracking (see Figure 6). The maximum flexion error is 0.75° . Its mean is 0.15° . In general, the multi-force control behaves less stable than the contact control does in the other scenario. The force error increases during quicker actuation of the flexion angle compared to non- or low-actuated periods. During the low velocity periods, the force error is reduced to almost zero. All the important measures for this experiment and the concerning control parameters are summarized in Table 2.

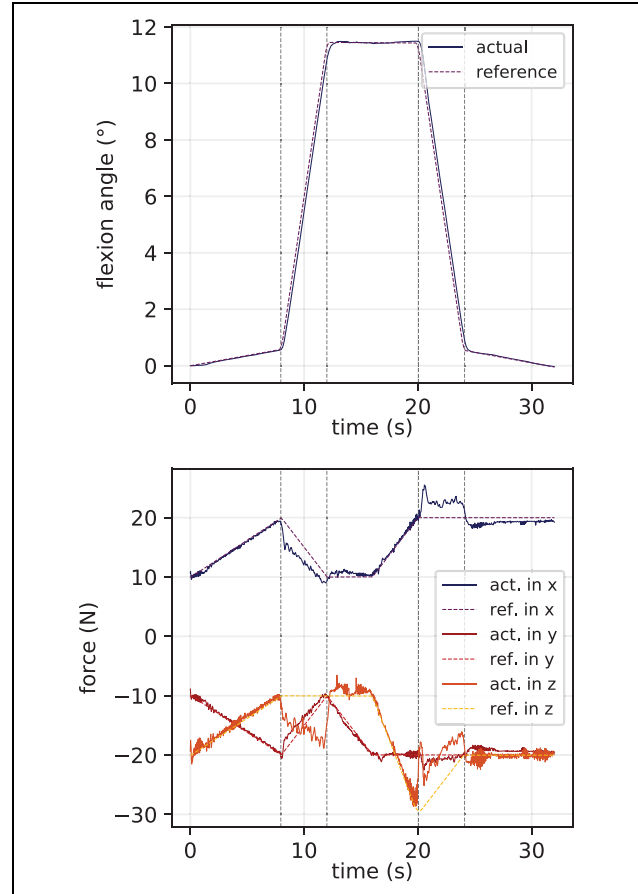


Figure 6. Flexion (above) and force tracking (below) of the multi-force control during the described task.

Comparison between position and force prioritization

In order to identify the influence of force and position prioritization, the previous experiment is repeated under force priority. The task trajectories for force and position control remain identical, yet the flexion is now pursued under null space. The forces are tracked as main task. As expected, this change leads to improved force tracking and less accurate rotation (see Figure 7). As before, the tracking deviations increase during quicker motions. The maximal and the mean force error is reduced significantly to 5.23 and 0.62 N. The position deviation increases moderately to a maximum of 1.45° and a mean of 0.38° . The following two points can be summarized regarding the prioritization:

- For force prioritization, the force errors remain very low and independent of the position related task. On the other hand, the position errors are especially high during active movement, as the actual control velocity is filtered by the null space matrix.
- Position prioritization on the opposite performs significantly better regarding the position related tasks.

Table 2. Parameter and quality measures of the multi-force control experiment.

Parameter	Value	Unit
Control frequency	4000	Hz
PT1-Force filter constant	0.1	s
Max. ref. angular velocity	2.75	deg s ⁻¹
PT2-Stiffness c	250,000	N m ⁻¹
PT2-Damping d	20	
PT2-Time constant T	0.2	s
Quality measure	Value	Unit
Position accuracy	<0.01	deg
Force accuracy	<0.1	N
Maximum rotation error $ \delta x _{\max}$	0.75	deg
Mean rotation error $ \delta x _{\text{mean}}$	0.15	deg
Root mean square rotation error RMS δx	0.27	deg
Maximum Euclidean force deviation $\ \delta f\ _{\max}^2$	11.58	N
Mean Euclidean force deviation $\ \delta f\ _{\text{mean}}^2$	2.29	N
Root mean square force deviation RMS δf	3.36	N

Table 3. Quality measures of multi-force control with position prioritization compared to force prioritization.

Quality Measure	Position Prioritization	Force Prioritization	Unit
$ \delta x _{\max}$	0.75	1.44	deg
$ \delta x _{\text{mean}}$	0.15	0.38	deg
RMS δx	0.27	0.67	deg
$\ \delta f\ _{\max}^2$	11.58	5.22	N
$\ \delta f\ _{\text{mean}}^2$	2.29	0.62	N
RMS δf	3.36	0.81	N

Bold values represent the primary regulation targets.

The mentioned quality measures are summarized in Table 3.

Conclusion

In this publication, two new compliant control architectures were introduced based on null space exploitation: contact and multi-force control. They are capable of handling interaction tasks with partially or fully coupled unknown non-linear systems.

In contrast to some established methods, Jacobian inversion is avoided and no affection by inner singularities occurs. By separating either force or position tasks from the original task space to null space, a redundancy is created that is exploited to increase the robustness and stability of the kinematic velocity projections.

Only few parameters had to be adjusted due to the one-dimensional contact space projections. In consequence, less system parameters are required as for impedance or hybrid control. In addition, Sygulla et al. showed that with the design of appropriate observers parameter tuning can be reduced even further.³⁴

The introduced control schemes avoid cross couplings when compared to the classical hybrid approaches.² The usage of the null space matrix ensures a clear orthogonal split between position and force control. Therefore, the force- and position-driven joint velocities do not interact with each other. The described multi-force solutions offer the opportunity to emphasize either the position or the force task. Depending on the choice of the primary control portion, the secondary goal is pursued in null space. Consequently, the primary goals always prevail. The use of force prioritization offers an interesting approach to control the robot in any direction while remaining stable.

Acknowledgements

The authors would like to thank Fritz Seidl, MA, for interpreting and translating, and proofreading and language editing this manuscript. Furthermore, the authors would like to thank M.Sc. Felix Sygulla and Dr-Ing. Christoph Schütz, who introduced us to null space solutions. Finally, the authors would like to thank Prof. Dr Daniel Rixen for the supervision of Nikolas Wilhelm's semester thesis, which lead to this control idea and Univ.-Prof. Dr med.

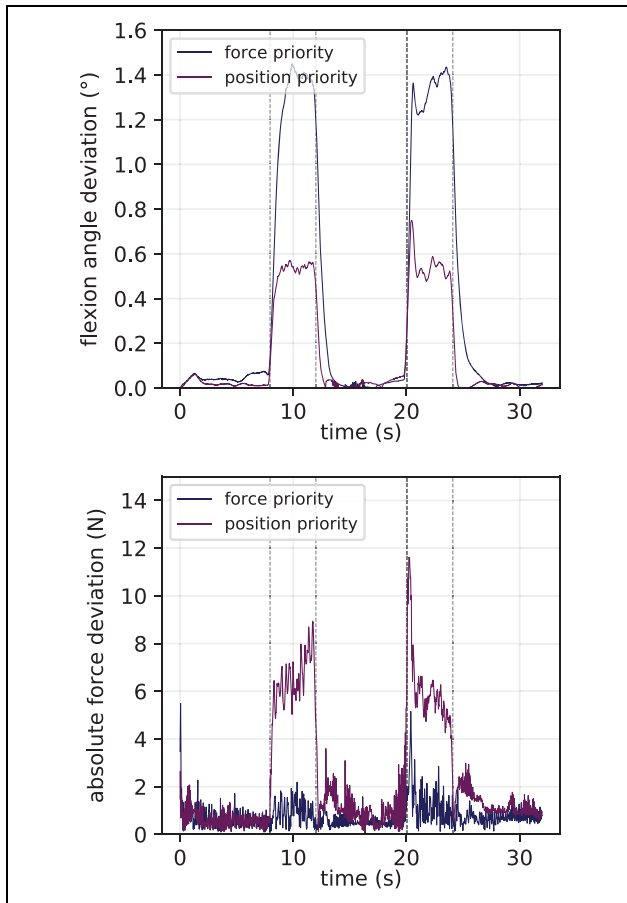


Figure 7. Comparison of the tracking capabilities between position- and force-prioritized multi-force control. The position-errors are shown above. The Euclidean norm of the force error is illustrated below.

Still, the position error increases proportional to the velocity of the task. As expected, the force errors are significantly higher than with force prioritization.

Rüdiger von Eisenhart-Rothe for giving us the opportunity to work in orthopaedic research.

Declaration of conflicting interests

The author(s) declared no potential conflicts of interest with respect to the research, authorship, and/or publication of this article.

Funding

The author(s) disclosed receipt of the following financial support for the research, authorship, and/or publication of this article: This work was supported by the German Research Foundation (DFG) and the Technical University of Munich (TUM) in the framework of the Open Access Publishing Program.

ORCID iD

Nikolas Wilhelm  <https://orcid.org/0000-0003-3352-2895>

Constantin von Deimling  <https://orcid.org/0000-0002-7633-6622>

Supplemental material

Supplemental material is available online with this article.

References

- Leylavi Shoushtari A, Dario P and Mazzoleni S. A review on the evolvement trend of robotic interaction control. *Ind Robot* 2016; 430(5): 535–551.
- Raibert MH and Craig JJ. Hybrid position/force control of manipulators. *J Dyn Syst Meas Control* 1981; 1030(2): 126.
- Hogan N. Impedance control: an approach to manipulation: part II – implementation. *J Dyn Syst Meas Control* 1985; 1070(1): 8.
- Calanca A, Muradore R and Fiorini P. A review of algorithms for compliant control of stiff and fixed-compliance robots. *IEEE-ASME T Mech* 2016; 210(2): 613–624.
- Colgate JE and Brown JM. *Factors affecting the z-width of a haptic display*. In: *Proceedings of the 1994 IEEE international conference on robotics and automation*, San Diego, CA, USA, 8–13 May 1994, pp. 3205–3210. Piscataway, NJ, USA: IEEE Computer Society Press.
- Roveda L, Pedrocchi N and Tosatti LM. Exploiting impedance shaping approaches to overcome force overshoots in delicate interaction tasks. *Int J Adv Robot Syst* 2016; 130(5): 172988141666277.
- Walker ID. *The use of kinematic redundancy in reducing impact and contact effects in manipulation*. In: *Proceedings*, 1990, pp. 434–439. Los Alamitos, Calif and Piscataway, NJ: IEEE Computer Society Press.
- Khatib O. A unified approach for motion and force control of robot manipulators: the operational space formulation. *IEEE J Robot Autom* 1987; 30 (1): 43–53.
- Fisher WD and Mujtaba MS. Hybrid position/force control: a correct formulation. *Int J Robot Res* 1992; 110(4): 299–311.
- Baerlocher P and Boulic R. An inverse kinematics architecture enforcing an arbitrary number of strict priority levels. *Visual Comput* 2004; 200(6): 402–417.
- Nakanishi J, Cory R, Mistry M, et al. Operational space control: a theoretical and empirical comparison. *Int J Robot Res* 2008; 270(6): 737–757.
- Antonelli G. Stability analysis for prioritized closed-loop inverse kinematic algorithms for redundant robotic systems. *IEEE T Robot* 2009; 250(5): 985–994.
- Decre W, Smits R, Bruyninckx H, et al. *Extending iTaSC to support inequality constraints and non-instantaneous task specification*. In: *2009 IEEE international conference on robotics and automation*, Kobe, Japan, 12–17 May 2009, pp. 964–971.
- Kanoun O, Lamiroux F and Wieber P. Kinematic control of redundant manipulators: generalizing the task-priority framework to inequality task. *IEEE T Robot* 2011; 270(4): 785–792.
- Albu-Schaffer A, Ott C, Frese U, et al. *Cartesian impedance control of redundant robots: recent results with the DLR-light-weight-arms*. In: *2003 IEEE international conference on robotics and automation (Cat. No. 03CH37422)*, Taipei, Taiwan, 14–19 September 2003, vol. 3, pp. 3704–3709.
- Khatib O, Sentis K, Park J, et al. Whole-body dynamic behavior and control of human-like robots. *Int J Hum Robot* 2004; 10: 29–43.
- Sentis L and Khatib O. Synthesis of whole-body behaviors through hierarchical control of behavioral primitives. *Int J Hum Robot* 2005: 505–518.
- Mansard N, Khatib O and Kheddar A. A unified approach to integrate unilateral constraints in the stack of tasks. *IEEE T Robot* 2009; 250(3): 670–685.
- Dietrich A, Albu-Schäffer A and Hirzinger G. *On continuous null space projections for torque-based, hierarchical, multi-objective manipulation*. In: *2012 IEEE international conference on robotics and automation*, Saint Paul, MN, USA, 14–18 May 2012, pp. 2978–2985.
- Sadeghian H, Villani L, Keshmiri M, et al. Dynamic multi-priority control in redundant robotic systems. *Robotica* 2013; 310(7): 1155–1167.
- Dietrich A, Ott C and Albu-Schäffer A. An overview of null space projections for redundant, torque-controlled robots. *Int J Robot Res* 2015; 340(11): 1385–1400.
- Schuetz C, Pfaff J, Sygulla F, et al. *Motion planning for redundant manipulators in uncertain environments based on tactile feedback*. In: *IEEE/RSJ international conference on intelligent robots and systems*, 28 September 2015–2 October 2015, Hamburg, Germany, pp. 6387–6394.
- Sandoval J, Poisson G and Vieyres P. *A new kinematic formulation of the RCM constraint for redundant torque-controlled robots*. In: *2017 IEEE/RSJ international conference on intelligent robots and systems (IROS)*, Vancouver, BC, Canada, 24–28 September 2017, pp. 4576–4581.
- An C and Hollerbach J. *Kinematic stability issues in force control of manipulators*. In: *Proceedings. 1987 IEEE international conference on robotics and automation*, Raleigh, NC, USA, 31 March–3 April 1987, pp. 897–903. Piscataway, NJ, USA: Institute of Electrical and Electronics Engineers.

25. Zhang H. *Kinematic stability of robot manipulators under force control*. In: *IEEE international conference on robotics and automation*, '89, May 1989, Los Alamitos, pp. 80–85. Piscataway, NJ, USA: IEEE Computer Society Press.
26. Liégeois A. Automatic supervisory control of the configuration and behavior of multibody mechanisms. *IEEE Trans Syst Man Cybern* 1977; 70(12): 868–871.
27. Nemeč B and Zlajpah L. Force control of redundant robots in unstructured environment. *IEEE Trans Ind Electron* 2002; 49(1): 233–240.
28. Sadeghian H, Keshmiri M, Villani L, et al. *Null-space impedance control with disturbance observer*. In: *2012 IEEE/RSJ international conference on intelligent robots and systems*, ilamoura, Portugal, 7–12 October 2012, pp. 2795–2800. Piscataway, NJ, USA: IEEE.
29. Park J and Khatib O. Robot multiple contact control. *Robotica* 2008; 26(05): 126.
30. Platt R, Abdallah M and Wampler C (eds) *Multiple-priority impedance control*. In: *ICRA*, 9–13 May 2011, Shanghai, China. Piscataway, NJ: IEEE.
31. Gertz MW, Kim JO and Khosla PK. *Exploiting redundancy to reduce impact force*. In: *Intelligent robots and systems '91: Proceedings IROS '91*, Osaka, Japan, 3–5 November 1991, New York, pp. 179–184. Piscataway, NJ, USA: Institute of Electrical and Electronics Engineers.
32. Chung WJ, Kim IH and Joh J. Null-space dynamics-based control of redundant manipulators in reducing impact. *Control Eng Pract* 1997; 50(9): 1273–1282.
33. Whitney D. Resolved motion rate control of manipulators and human prostheses. *IEEE T Hum-Mach Syst* 1969; 100(2): 47–53.
34. Sygulla F, Schuetz C and Rixen D. *Adaptive motion control in uncertain environments using tactile feedback*. In: *International conference on advanced intelligent mechatronics (AIM)*, Banff, AB, Canada, 12–15 July 2016, pp. 1277–1284. Piscataway, NJ, USA: IEEE.
35. Stewart GW. On the perturbation of pseudo-inverses, projections and linear least squares problems. *SIAM Review* 1977; 19(4): 634–662.